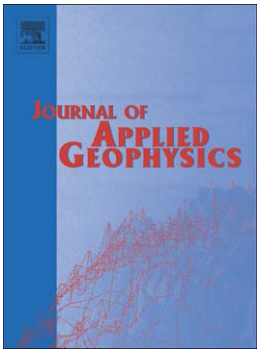

Geomorphological and geophysical investigations for the characterization of the Roman Carsulae site (Tiber basin, Central Italy)

C. Bottari, D. Aringoli, R. Carluccio, C. Castellano, F. D'Ajello Caracciolo, M. Gasperini, M. Materazzi, I. Nicolosi, G. Pambianchi, P. Pieruccini, V. Sepe, S. Urbini, F. Varazi

PII: S0926-9851(17)30315-4
DOI: doi:10.1016/j.jappgeo.2017.03.021
Reference: APPGEO 3276

To appear in: *Journal of Applied Geophysics*

Received date: 4 July 2016
Revised date: 29 March 2017
Accepted date: 30 March 2017

Geomorphological and geophysical investigations for the characterization of the Roman Carsulae site (Tiber basin, Central Italy)

C. Bottari[1], D. Aringoli[2], R. Carluccio[1], C. Castellano[1], F. D'Ajello Caracciolo[1], M. Gasperini[3], M. Materazzi[2], I. Nicolosi[1], G. Pambianchi[2], P. Pieruccini[4], V. Sepe[1], S. Urbini[1], F.Varazi[5]

[1] *Istituto Nazionale di Geofisica e Vulcanologia, via di Vigna Murata 605, 00143 Roma,*
[2] *Scuola di Scienze e Tecnologie, Viale Gentile III da Varano, 62032 Camerino.*
[3] *Associazione per lo Studio del Territorio, la Ricerca e l'Archeologia, Terni.*
[4] *Dipartimento di Scienze Fisiche, della Terra e dell'Ambiente, Via Laterina, Siena.*
[5] *Geolab, Museo di Scienze della Terra di San Gemini, San Gemini.*

Abstract

This paper aims to bring to light the possible linkage between karstic phenomena and the human occupation of the Roman site of Carsulae (Tiber basin, Central Italy). Dolines are a typical morphological expression of karst rocks dissolution and collapse and, usually, they represent a potential hazard for human activities and, in particular, in the care and maintenance of cultural heritage sites. In this study, we observed that the development of a subsidence doline caused severe damage to some archaeological structures at Carsulae monumental site. According to the results obtained in our investigation, three sites at least with karst dissolution phenomena in the shallow calcareous tufa layer have been identified. One of them subsided probably in Roman times and produced a sharp deformation of the decumanus. In order to understand the evolution of this territory an integrated geomorphological and geophysical survey was carried out. The combination between the information derived from different geophysical techniques, such as: Electrical Resistivity Tomography (ERT), Frequency-Domain Electromagnetism (FDEM), Ground Penetrating Radar (GPR) clearly pointed out that the calcareous tufa layer is characterized by an irregular geometry and resulted affected by karst dissolution in several parts of the investigated area.

Four boreholes opportunely located, provided direct information about the depth and the alteration of the calcareous tufa basement and precious calibration data for the geophysical methods.

This study contributes to improve our knowledge on the evolution of the Carsulae archaeological site providing a new insight into the adaptation of ancient human societies in this problematic territory.

Key words: Geomorphological evolution, geophysical investigations: ERT and FDEM, GPR, Roman archaeological site, karst processes, Central Italy

1. Introduction

Ancient settlements had always strict relationship with local geomorphology and landforms as they were of essential economic significance for thousands of years. In particular, the karst landforms offered important settlement locations of high palaeoenvironmental interest (Bruxelles, 2001). Dolines and karst landforms represented a favorable location for human activity for agriculture, resource extraction, quarrying and mineral exploitation, pottery and water resources. Many ancient cities depended on karst geology for their water (Crouch, 1993). The karst terrains are characterized by extreme rate of changes due to its natural dynamical evolution representing a potential hazard for human activities. These latter could in turn produce an important impact on the karst environment equilibrium.

The settlement of Carsulae, an ancient Roman city in Central Italy, was built in the third century BC in a strategic position along the consular Flaminia road, in a karstic environment characterized by dolines and limestone dissolution morphologies; at Carsulae a large karstic landform was used to host an important building like the Roman amphitheatre (Fig.1 a). A small doline, located to the north of the decumanus road, partially collapsed during the city history, as evidenced by the deformation and re-building of the road (Fig.1b). This episode was ascribed to seismic events by Bonini et al. (2003), whereas other studies rejected this hypothesis (Aringoli et al., 2009; Bottari and Sepe, 2013).

This study is furthermore focused on the comprehension of the relationship between the settlement of Carsulae and its karstic environment and how these evolving landforms could have interacted with the human settlement. Based on specific and updated/revised archaeological studies, an integrated geological, geomorphological and geophysical survey was carried out at the Carsulae archaeological site. In particular, this study exploits the advantage of combining geological, geomorphological and geophysical information for karst structure characterization (Chalikakis et al., 2011).

Based on specific and updated/revised archaeological studies, the integrated approach was made up of: four geognostic boreholes, five Electrical Resistivity Tomography (ERT) profiles, two Ground Penetrating Radar (GPR) profiles and Frequency-Domain Electro-Magnetic (FDEM) surveys.

The obtained results pointed out the general condition of the calcareous tufa basement, on which archaeological ruins lie, revealing its high alteration/dissolution status due to the groundwater circulation. In particular, we focused on the characterization of the doline located to the north of the decumanus since it represents a clear evidence of the dynamic interaction between an evolving karst system and a human settlement.

2. Historical and archaeological data

The Roman site of Carsulae was built at the base of Martani Ridge in a strategic geographic position along the Consular Flaminia road characterized by the presence of healthy-water sources and a fertile soil (Fig.1). The importance of this site was testified by different historical sources (Strabo, Pliny the Younger, and Tacitus) and Carsulae had also a strategical military position being placed on the main road used for connecting Rome to the Umbria region and to the Adriatic coast. The foundation of Carsulae dates back to 3rd century BC in conjunction with the construction of the Consular Flaminia road (Ciotti, 1976; Bruschetti, 1995; Morigi, 1997; Angelelli, 1998), the western tract of the road runs to the west of Martani Mts and links Narnia with *Forum Flamini*, crossing through *Carsulae*. The first building phase of Carsulae occurred in the Republican period (3rd century BC-1st century BC) and it is poorly known. Since 27 BC (Augustan period), a phase of monumental and urban change is attested in the area which hide the previous phases; the town of Carsulae was transformed into a municipium, quickly expanding its limits and showing a prosperous development. Besides, in Augustan period (27 BC to 14 AD) the Consular Flaminia road was restored. In the Imperial

period (from the 1st to the 4th cent. AD), Carsulae site was still characterized by a flourishing status as attested by epigraphs. The gradual abandonment of the site started in the fourth century AD linked also to the decline of the western track of the Consular Flaminia road, gradually replaced with the eastern one (Angelelli, 1998). Its abandonment is coincident with the lack of epigraphic sources (Morigi, 1997).

Archaeological site excavations carried out in the 70's revealed the presence of several buildings erected along the Flaminia road, which crosses the city in a S-N direction (Ciotti, 1976). In the central sector it passes through the Roman Forum where are still visible the remains of the twins temples and some public buildings. To the east of the Flaminia road are visible some rooms belonging to the market and the basilica, which entrance is placed in front of the Forum square. The decumanus, built perpendicularly to the Flaminia road in an east-west direction, gave access to the amphitheatre and the Roman theatre. To the north, along the Consular Flaminia road is placed the S. Damian Arch that is the northern entrance of the town.

2.1 Doline area

Among the dolines of the archaeological site, that one located between the Flaminia Consular road and the decumanus is worth noting (Fig. 1 a, b).

The decumanus runs along the southern border of the doline and it was sharply deformed by the doline collapse in its terminal portion of about 1.8 m (Ciotti, 1976; Bonini et al., 2003; Aringoli et al., 2009; Bottari and Sepe, 2013), it was subsequently repaired using a different type of paved floor.

Recent archaeological excavations carried out in the northern part of the doline ruled out that its collapse occurred during the final phase of the city (4th century A.D.). Moreover, some archaeological excavations conducted in 2013 near the northern border pointed out the presence of a paved floor probably belonging to the Republican period. The dig, furtherly broaden in 2014, evidenced that this road, underwent to some structural changes and was modified in the Augustan period (1st century BC-1st century AD). This period seems to correspond with the phase of monumental and urban change at Carsulae. Based on the archaeological data, the doline genesis would be contemporaneous to the foundation of the town. Consequently, the urban plan may be developed by adapting it to the surrounding environment of that time. Moreover, the gradual collapse of the doline could justify the deformation of the decumanus observed in the southern side, and may be related to the road changes of the northern side.

3. Geological and Geomorphological features

The Roman site of Carsulae is located at the foot of the western slope of the Martani Mts calcareous Ridge next to the West-Tiber tectonic basin, which is filled with Plio-Pleistocene sediments (Fig. 2a). The Tiber basin extends from Terni (to the south) to Borgo S. Sepolcro (northward from the study area; Coltorti and Pieruccini, 1997a, 1997b). Martani Mts Ridge subdivides the basin into two portions: West Tiber Basin (WTB) and East Tiber Basin (ETB). The WTB and ETB are both filled with fluvial deposits up to 500 m thick, and the sediments are late Early Pliocene in age and constitute the older terrestrial evidence. These represent a marker for the beginning of the Mountain Building and landscape evolution of the Umbro-Marchean Apennines. The structuring of this sector is dated to the Miocene (Deiana and Pialli, 1994), although the re-activation of the main overthrusts are referred to the Upper Messinian-Early Pliocene (Calamita et al. 1999; Coltorti and Pieruccini, 1997b). The western slope of the Martani Ridge is a fault escarpment related to the presence of a high-angle trastensive to normal fault system with cumulative displacements up to 1000 m

(Barchi et al., 1991; Calamita and Pierantoni, 1994). The origin of the WTB was interpreted as a graben (Ambrosetti et al., 1978; Basilici, 1997) or semi-graben (Barchi et al., 1998). However, stratigraphical evidence as well as structural studies provided evidence for a compressional origin of the Pliocene Basin as a synform or satellite (piggy-back) basin (Boccaletti et al., 1995; Bonini, 1998; Coltorti and Pieruccini, 1997b). These are associated to compressional regime or to the superficial folding related to a deep detachment along the east-dipping low angle normal faults (Calamita et al., 1999). The WTB sedimentary sequence is made up of late Early-Middle Pliocene clays, silts and sands with lignites beds deposited in lakes, swamps, deltas, alluvial fans and ribbon channels (Basilici, 1997). The Early Pleistocene sequence lies unconformably on the older deposits made up of coarser-grained facies typical of wandering to meandering rivers (Ambrosetti et al., 1995; Basilici, 1997). Middle Pleistocene carbonate-rich sediments unconformably overlie the older units and are found all along the fault escarpment (Ambrosetti et al., 1995). These are calcareous tufa with complex geometries, deposited in shallow lakes and fluvial systems (Chafetz and Folk, 1984). The morphology of the area is mainly linked to geomorphological, neotectonic, depositional and erosional events that affected the fault slope of the Martani Mts, which is characterized by well-developed morphostructural evidence (i.e. triangular and trapezoidal facets) indicating recent extensional movements (Leeder and Gawthorpe, 1987). Sinkholes, dolines and karst depressions of different shapes and dimensions characterize the area (Fig.2b). Field surveys allowed the identification of numerous landforms, deposits and processes mainly associated to gravitational, fluvial and karstic processes. The karstic deposits are evident at the site scale and consist of calcareous tufa, deposited within marsh and spring environments at the foot slope of the fault escarpment. Their origin is connected with groundwater circulation within the limestone complex of the Martani Ridge. Calcareous tufa therefore forms more or less continuous banks separated by few meters high scarps located at an elevation progressively lowering westwards, associated to systems of waterfalls and swamps prograding downslope.

Landforms associated to epigeous karst are represented by dolines locally with circular shape, some dozen of meter up to one hundred meter wide and a few meter deep (Fig.2b). Wide and deep depressions associated to coalescent circular or slightly elongated dolines have been also recognized; they have been affected by surface erosional processes or by human activity. Some of them are filled by recent fine-grained deposits coming from the slopes. Sinkholes formed as the result of the collapse of the roofs of underground cavities.

3.1. Geological Borehole

In order to provide a direct image of the shallow (from 10 to 30 m depth) soil conditions four geognostic boreholes (S1, S2, S3 and S4, see Figs 3, 4) were placed and carried out in different points of the archaeological site. The cores analysis permitted to achieve information about the physical status (continuity, consistency, alteration, weathering) of the calcareous tufa deposits.

The S1, S2 and S3 boreholes showed evident similarities while the S4, drilled on the bottom of the doline, provided very different results (Fig. 4).

At the base of calcareous tufa a layer of a silty and clayey sands with thin layers of fine alluvial gravels (*Santa Maria di Ciciliano Unit*-early Pleistocene) was found at about 27 m depth in the S2 borehole (Fig. 4). The sequence of calcareous tufa obtained by S1, S2 and S3 boreholes is made up of calcareous silts and sandy silts, very porous, high to low cemented where the sandy fraction is more abundant. Conversely, if the clayey fraction increases the concretions of

Fe/Mn may be present. Besides, sub-rounded clasts of calcareous tufa and calcareous elements of the *Umbria-Marche Succession* are very rare (Centamore and Deiana, 1986) while thin levels of dark gray to light brown plastic clay are intercalated. Within the same sequence, buried and undeveloped paleosoils are present. The sedimentation, as mentioned before, occurred in environment characterized by cold waters, richness in calcium carbonate, low energy, and by the presence of ponds and marshes. The uppermost portion of the calcareous tufa is weathered into a soil sequence consisting of two buried paleosols and the present soil. The agricultural horizon in the present soil contains pottery fragments and scrambled plant remains, about 1 m thick. In the S1 borehole, two clayey horizons and a thin carbonate horizon have been recognized. The presence of the buried clayey horizon at the bottom suggests the truncation of the previously formed paleosoil. The latter buries another undeveloped paleosoil made up of a clayey horizon, with abundant siliceous skeleton, well-developed above a thick calcareous horizon.

In the S2 borehole, this horizon is made up of a completely siliceous skeleton. A chronological attribution of the last events has been attempted in order to characterize depositional history of the site. The most recent paleosoils are C1 and C1/ 3 samples in the S1 borehole and the C2/2 sample in the S2 borehole. Radiocarbon dating using Accelerator Mass Spectrometry (AMS) has provided different results reported in Table 1.

The paleosoil sequence suggests that the sedimentation of alluvial deposits occurred after that of calcareous tufa. The former have been later weathered into an oldest paleosoil, whose characteristics suggest a well-vegetated environment and a long time geomorphological stability of the topographic surface. As a consequence, the carbonate fraction was completely leached out, leaving the siliceous fraction as residue. The pedogenetic phase was interrupted and the soil was partially truncated (surface horizons are definitely absent) and colluviated. This indicates a phase of instability of the topographic surface with degradation of the vegetation cover that triggered important soil erosion processes. The formation of the second paleosoil, which is also truncated and less developed than the previous one, occurred subsequently. Finally, the present soil shows evidence of leaching out with precipitation of carbonates in the deepest horizons, in addition to evidence of human impact related to agricultural practices.

The S4 borehole, drilled on the bottom of the doline bordering northward the decumanus, shows a very different sequence (Fig. 3). Below the present soil, slope and colluvial deposits of different size and nature (calcareous tufa and/or bedrock fragments) containing abundant pottery fragments have been found up to a depth of about 3.70m. From this point up to the end of the borehole (roughly 10m), the grain size tends drastically to decrease, very dark and plastic clayey levels containing abundant organic matter and ceramic fragments are, whose frequency tends to decrease with the depth.

4. Geophysical investigations

In recent years, several studies were undertaken in order to provide guidelines for the application of geophysical methods in karst system exploration (Chalikakis et al., 2011 and reference therein). Several geophysical techniques could be properly used considering the strong contrast in physical properties between void, or infilling material, and the karst rock (Gibson et al., 2004; Leucci et al. (2004); El-Qady et al., 2005; Margiotta et al., 2012). Among them, some of the most frequently used are the ERT tomography and the GPR but also other methods can provide very useful information as well.

In order to achieve a more detailed image of the possible relationship between the geomorphologic assessment of the area and the Carsulae site history an integrated geophysical survey was carried out in the archaeological site (Fig. 3). In particular, the main goal was to identify the calcareous tufa layer trying to assess its state of alteration. To pursue this

objective, we used the following geophysical methods: Electrical Resistivity Tomography (ERT); Frequency-Domain Electromagnetism (FDEM) and Ground Penetrating Radar (GPR). In addition four boreholes were properly placed (Fig. 3) and carried out in the investigated area providing also calibration information for the geophysical methods.

The ERT is based on induction of a current through direct coupling of electrodes inserted into the ground. Two separate electrodes are used to measure the potential difference over the circuit. Using Ohm's Law and the geometry of the used electrode configuration, the resistivity (or in the case of non-homogeneous material, apparent resistivity) can be calculated. The equipment used was a SYSCAL Pro 10 channel (IRIS instruments) equipped with 72 electrodes and measurements were carried out using Wenner–Dipole dipole arrays in order to preserve a good compromise between vertical and horizontal shape of retrieved anomalies (Table 2; Loke, 2012). For the inversion of apparent resistivity data an algorithm based on a deconvolution method of minimum squares was used (software TomolaB; www.geoastier.com), which allows to obtain 2D sections through calculation modules to finite elements, taking also into account the topographical corrections.

FDEM survey is based on the induction of eddy current loops in the ground by introducing an alternating current in the transmitter coils. The intensity of the induced eddy currents is directly proportional to the terrain conductivity in the proximity of the loops. The induced current generate a secondary magnetic field that is proportional to the value of the primary field. A receiver coil placed at a specific distance from the transmitter can measure the secondary magnetic field both in quadrature (90° out of phase) and in in-phase components, with respect to the primary field. The quadrature value is related to the ground conductivity characteristics (in milliSiemens per meter), while the in-phase component (measured in parts per thousands or millions) is significantly more sensitive to the presence of metallic objects.

The electromagnetic induction method measures the conductivity variations of the most superficial part of ground. Strong anomalous values of ground conductivity can be addressed to presence of: archaeological buried remains, ground stratifications or alterations, water or conductive fluids. We used a Geonics EM31-MK2 system (operating frequency, 9.8 KHz; intercoil spacing, 3.66 m), which offers averaged measures of ground conductivity variations of the first 6 m depth (as horizontal dipole mode). FDEM investigated areas are reported as red dots boxes in figure 3.

The GPR method is based on the reflection of electromagnetic waves generated at the interface between media characterized by differences in dielectric properties. The use of antennas with different frequencies allows to investigate the subsoil at different depths and with different resolutions. In this study we used a GSSI Sir3000 instrument equipped with a 20 MHz bistatic antenna and a 200 MHz monostatic antennas. The GPR profiles were geo-referenced by the coupling of a D-GPS acquisition. The obtained radargrams were corrected for the topography (where needed) and processed by horizontal and vertical filtering and gain compensation. Time to depth conversion were performed through the analysis of hyperbola diffractions which pointed out an averaged electromagnetic wave speed of about 0.07 m/ns in the weathered shallow soil (Table 3).

Where possible the measures were planned in order to achieve results comparison to maximize the significance of the measurements and to reduce the ambiguities associated with each of the geophysical methods.

5. Geophysical survey main results

5.1 ERT profiles

The five ERT profiles were placed in the archeological area according to different objectives (see Fig. 5, Table 2). The ERT1, ERT3 and ERT4 were aimed to achieve a deep image of calcareous tufa status maximizing at the same time the site coverage. The ERT2 was planned in order to achieve more detailed information of the doline structure while the ERT5 was placed in the Roman Forum area where the FDEM survey returned a circular shaped conductive anomaly.

The ERT1 profile runs from north to south along the main road to access the site and the electrical model reveals the presence of some high resistivity lithoid bodies ($\rho > 180\ \Omega m$). The superficial ones are referable to calcareous tufa and lie on high conductive silty-clayey matrix (Fig. 5a). Along this profile the calcareous tufa layer appears discontinuous in the whole investigation range suggesting the presence of a large karstic altered zone.

The ERT2 profile (Fig. 5b) shows a concave up resistive layer ($55<\rho<90\ \Omega m$) interbedded in a more conductive material ($9<\rho<20\ \Omega m$), that marks the collapsed area. The resistive layer is interrupted in its deep part (from 45 to 51 m along the profile) indicating the maximum subsidence area of the doline. Besides, along the first ten meters of the profile a superficial high resistive anomaly occurs which could be linked to the presence of archeological remains as evidenced by recent exploration digs. The S4 borehole (placed at about 38 m from the profile start) shows a stratigraphic succession made up of soil lying on debris material with fragments of calcareous tufa (at about 4m of depth) and silt and clay up to the end of borehole. The coarse debris material (from 1 to 4m of depth) could be considered consistent with the ERT2 resistive layer.

The ERT3 profile (Fig. 5c), elongated to the W-E direction, crosses the archeological site almost perpendicularly to the ERT1 and ERT2. It shows a 10 m thick resistive layer (calcareous tufa) interrupted by a conductive zone ($\rho \sim 20\ \Omega m$) in the central part of the profile, between the progressive distances of 140 and 200 meters and in correspondence of the collapsed doline. This low-resistivity area appears as an electrically homogenous vertical body up to 60 m depth probably indicating a deeper origin of this karstic depression. Along the ERT3, the S3 borehole is placed at about 260 m from the profile beginning and it shows a stratigraphic succession made up of sands, calcareous tufa and clays. The thickness and depth of the calcareous tufa layer is consistent with the resistive anomaly ($\rho \sim 200\Omega m$) occurring between the progressive distance 210-260 m.

The ERT 4 profile (Fig. 5d) was performed eastward the Roman theatre and close to the S1 and S2 boreholes. It indicates the presence of a well-defined resistive ($\rho \sim 350\ \Omega m$) layer (calcareous tufa) between the progressive distances of 120-300 m which is placed at about 4 m depth. Also the layer thickness varies, along the profile, from 10 m up to more than 40 m. The low-resistivity material ($\rho < 37\ \Omega m$) that surrounds the resistive layer appears compatible with the clayey-silty material. The S1 borehole is positioned at about 170 m from the beginning of the line and it showed a succession of fine sands layers (up to 4 m from surface) followed by a thick strata of calcareous tufa. These results strongly support the correct interpretation of the electrical stratigraphy. The S2 borehole, placed northward to the previous one (progressive distance=330 m) figured out a succession of calcareous tufa with sandy and travertine silt layers, sandy silts water-saturated, calcareous tufa sands with silty-clayey material. The sandy and silty alternation could be considered consistent with the conductive material ($\rho < 37\ \Omega m$) resulting in the electrical stratigraphy. Besides, the interruption of the resistive layer occurred between the progressive 70 and 100 meters could indicate the possible presence of a karstic dissolution phenomena that still has not produced a visible effect on the surface morphology.

Finally, the ERT 5 electrical stratigraphy (Fig. 5e) shows a high resistivity area ($\rho > 200\ \Omega m$; ascribable to the calcareous tufa layer) interrupted between the progressive distance 13-38 m by a high-conductive area ($\rho < 50\ \Omega m$).

This low-resistivity body is characterized by an increase in thickness from 4 m (at 13 m along the profile) up to 7 m (at 30 m). It is worthy to note that, between the progressive distances 33 and 38 m, it is characterized by close-to-vertical limits and its thickness exceed the investigation range (10 m). Similarly to the previous cases, we considered this conductive body made up of material resulting from the dissolution of calcareous tufa without any topographic expression on the surface.

5.2 FDEM survey

Some parts of the Carsuale archaeological site were surveyed using FDEM method with different objectives: i) to map the superficial extension and alteration degree of the calcareous tufa layer; ii) find out the presence of buried archaeological remains. Figure 6 reports the maps of ground conductivity points distribution obtained through the survey. As reported in the method description, the FDEM measures the averaged conductivity (the inverse of resistivity) of a shallow portion of ground (about 6 m) between the two coils.

The ERT profiles and boreholes highlighted a shallow stratigraphy made up of calcareous tufa (resistive), material resulting from the its dissolution and succession of clayey-silty material (conductive). On the base of these results, we interpreted the lower conductivity FDEM measures as due to the shallow presence of not-weathered calcareous tufa while the high-conductivity values as due to a thick layer of clayey-silty material.

The conductivity map obtained in the Antiquarium and Roman Forum area clearly showed the investigated area as characterized by the large presence of shallow, and probably compact, calcareous tufa. Two main anomalies occurred in this area showing differences in shape and conductivity values. In the Antiquarium area, the geometrical structure of the anomaly and the homogeneous conductivity values suggested its origin due to the presence of a buried archaeological structure (black dots box). In the Roman Forum the anomaly area was characterized by a circular shape and high conductivity values. The comparison between this anomaly and the ERT5 profile (Fig. 7) lead to ascribe its origin to the karst dissolution of the calcareous tufa and permitted to draw a 3D image where spatial extensions of the structure was provided by the FDEM measures and the third dimension (depth) was provided by the ERT profile.

The FDEM survey conducted in the doline area showed higher averaged conductivity with the highest values occurring in coincidence with the interruption of the resistive layer described in the ERT2 profile (see Figs. 5b, 7). The low-conductivity anomaly following the northern doline border had to be related to the presence of a paved floor (probably belonging to the Republican period) pointed out by the nearby archaeological digs conducted in 2013.

In the Roman theatre area, the FDEM measures showed a large presence of shallow calcareous tufa layer interrupted in the middle part by higher conductivity values (Fig.6). This more conductive body was interpreted as the presence of material resulting from the dissolution of calcareous tufa layer (similarly to the ERT3 profile interpretation). In the upper (northern) part of this area we observed an elongated series of very low conductivity values that could belong to some buried archaeological structure.

The survey conducted in the southern part of the area was more difficult to interpret. In this area the calcareous tufa layer appeared shallow and compact only in some parts while an alignment of high-conductivity measures, elongated in the NNW-SSE direction, could indicate a water drainage from the tanks discovered in the nearby wood.

5.3 GPR profiles

The two GPR profiles carried on in the archaeological area were characterized by different operative frequency in order to achieve information at different depth and detail.

The GPR1 profile was acquired using a bistatic 20 MHz antenna operated at discrete point with a signal stacking of 256 traces. It was located in the doline area close to the ERT2 profile (Fig. 8a) and the results comparison (Figs. 8b and 8c) showed a very good accord. Along the GPR1 profile was possible to observe a shallow reflection (red dots line) that deepen from the line start till the progressive distance of 50 m where it was interrupted generating also signal diffractions. The same reflection appeared again at progressive distance of 57 m showing strong similarity with the ERT2 resistive layer behavior. We thus interpreted it as generated from the top of the calcareous tufa layer.

The GPR2 profile was carried out using a monostatic antenna at 200 MHz frequency in continuous mode and partially overlapping the ERT1 profile along the road to access the site (Fig. 9a). The main target of the profile was to provide information about the presence and the density (intended as number of structures for meters of profile) of archaeological buried structures that could lead to a misleading interpretation of the shallow resistive layer in ERT1profile (Fig. 9b) . The GPR2 profile showed two similar and separate deep anomalies (white dots boxes in Fig. 9c), centered at progressive distance of 15 m and 35 m and occurring at 2 m and 1.5 m depth respectively. These two anomalies, probably related to the presence of relatively large buried structures, seemed to correspond to the shallow high resistivity values in the ERT1 profile (white dot boxes in Figs. 9a and 9b). Besides, the GPR2 radargram showed also the occurrence of many very shallow reflections that could be related to small masonry remains (red dots in Fig 9c). Although their density was quite high in some part of the profile, they seemed not to affect the resistivity values (also considering the electrodes spacing).

6. Conclusions

The main goal of this study was to assess the effectiveness of an integrated approach, based on geological, geomorphological and geophysical observations, for the characterization of a karst system trying to understand its impact on the ancient Roman Carsulae site. The integration between different geophysical methods returned a very clear image of the current state of the investigated area and the good overlay with stratigraphic data, obtained from geognostic boreholes, permitted to attempt a first reconstruction of recent geomorphological dynamics.

The integration between geophysical results (FDEM, GPR and ERT) and geomorphological observations pointed out that the calcareous tufa layer is characterized by an irregular geometry and resulted clearly affected by karst dissolution phenomena in large parts of the studied area.

The FDEM method allowed to define the presence, and its extent, of thick layers of clayey-silty material (conductive) contrasting the shallow not-weathered calcareous tufa (resistive values). For instance, in the Roman Forum, the comparison between the FDEM circular anomaly and the ERT5 profile well discloses the geophysical signature of the karst dissolution of the calcareous tufa in a combined 3D image (X-Y through the FDEM survey and Z by ERT profile). Furthermore, the ERT survey was able to recognize two main types of karst structures: those deeply rooted in the calcareous basement and those due to the dissolution of the shallow calcareous tufa layer. The first type revealed a marked geomorphological evidence in the area that was consciously tackled (i.e. the decumanus doline) or exploited (i. e. the amphitheatre site) by the Romans. The choice between tackling or exploiting the karst structures of the area probably depended on the recognition of being in the presence of an active or quiescent phenomena.

The investigations performed inside the doline area using ERT, FDEM and GPR, suggested its continuous collapse during the centuries. The quantity of work that Romans spent to remedy to its sinking is well testified by several

evidence such as the presence of filling materials containing various archaeological material (S4 borehole), the restoration of the decumanus and the presence of a paved road in the northern border of the doline, as highlighted by FDEM survey.

The GPR data provided useful and coherent information about the doline structure and could clarify, in a future investigation of the archaeological site, the relationship between the city architecture plan (through the mapping of buried structures) and the land development conditions.

In conclusion, this study introduces some new elements to better understand the evolution of the Carsulae territory and our knowledge of its archaeological site, providing also a new insight into the adaptation of ancient human societies in this problematic territory.

Acknowledgments

The authors wish to thank Carit Foundation that supported the research project. We also thank Dr. Calandra and Dr. De Angelis (Superintendence of the Archaeological Heritage of Umbria) for the precious and rewarding discussions regarding the site history and for the use of photographic material on the archaeological excavations.

References

Ambrosetti, P., Carboni, M.G., Conti, M.A., Sandrelli, F.,1978. Evoluzione paleogeografica e tettonica nei bacini tosco-umbro-laziali nel Pliocene e nel Pleistocene inferiore. Mem. Soc. Geol. It.19, 573-580.

Ambrosetti, P., Basilici, G., Capasso Barbato, L., Carboni, M.G., Di Stefano, G., Esu, D., Gliozzi, E., Petronio, C., Sardella, R., Squazzini, E., 1995. Il Pleistocene inferiore nel ramo sud occidentale del Bacino Tiberino (Umbria): aspetti litostratigrafici e biostratigrafici. Ital. J. Quaternary Sci 8, 19-36.

Angelelli, C., 1998. Carsulae. Il luogo e la memoria. In: Carsulae: la storia, la memoria, una esperienza didattica. Terni, 1998, 17-100.

Aringoli, D., Farabollini, P., Gentili, B., Materazzi, M., Pambianchi, G., 2009. Geomorphological evidences of natural disasters in the Roman archaeological site of Carsulae (Tiber basin central Italy). Belgeo: Revue Belge de Geographie, 5-20.

Barchi, M., Brozzetti, F., Lavecchia, G., 1991. Analisi strutturale e geometria dei bacini della media valle del Tevere e della Valle umbra. Boll. Soc. Geol. It. 110, 65-76.

Basilici, G., 1997. Sedimentary facies in an extensional and deep-lacustrine depositional system: the Pliocene Tiberino basin, Central Italy. Sediment. Geol. 109, 73-94.

Boccaletti, M., Bonini, M., Moratti, G., Sani, F., 1995. Le fasi compressive neogenico-quaternarie nell'Appennino settentrionale: relazioni con l'evoluzione dei bacini interni e con la tettonica del basamento. Stud. Geol. Cam. 1, 51-72.

Bonini, M., 1998. Chronology of deformation and analogue modelling of the Plio-Pleistocene 'Tiber Basin': implications for the evolution of the Northern Apennine (Italy). Tectonophysics 285, 147-165.

Bonini, M., Tanini, C., Moratti, G., Piccardi, L., Sani, F., 2003. Geological and archaeological evidence of active faulting on the Martana Fault (Umbria-Marche Apennines, Italy) and its geodynamic implications. J. Quaternary Sci. 18, 695-708.

Bottari, C., Sepe, V., 2013. The role of earthquakes, landslides and climate changes in the abandonment of the Roman Carsulae site (Tevere basin e Central Italy). Quatern. Int. 308-309, 105-111.

Bruschetti, P., 1995. Carsulae, Roma. Istituto poligrafico e Zecca dello Stato, 56 pp.

Bruxelles, L., 2001. Reconstitution morphologique du Causse du Larzac (Larzac central, Aveyron, France). Rôle des formations superficielles dans la morphogenèse karstique. Karstologia 38, 25-40.

Calamita, F., Coltorti, M., Pieruccini, P., Pizzi, A., 1999. Evoluzione strutturale e morfogenesi plio-quaternaria dell'appennino umbro-marchigiano tra il pedappennino umbro e la costa adriatica. Boll. Soc. Geol. It. 118, 125-139.

Calamita, F., Pierantoni, P.P., 1994. Structural setting of the southern Martani Mountains (Umbrian Apennines: central Italy). Mem. Soc. Geol. It. 48, 549-557.

Centamore, E., Deiana, G., 1986. La Geologia delle Marche. Studi Geologici Camerti. Volume Speciale, 145 pp.

Chafetz, H.S., Folk, R.L., 1984. Travertines: depositional morphology and the bacterially constructed constituents. J Sedim. R. 54 (1), 289-316.

Chalikakis k., Plagnes, V., Guerin R., Valois R., Boschet F.P., 2011. Contribution of geophysical methods to karst-system exploration: an overview. Hydrogeol J 19, 1169–1180.

Ciotti, U., 1976. Carsulae. In: AA.VV. San Gemini e Carsulae. Milano-Roma.

Coltorti, M., Pieruccini, P., 1997a. The southern East Tiber Basin (Spoleto, Central Italy): geology and stratigraphy of the Plio-Pleistocene sediments. Ital. J. Quaternary Sci. 10,159-180.

Coltorti, M., Pieruccini, P., 1997b. Middle-Upper Pliocene 'Compression' and Middle Pleistocene 'Extension' in the east Tiber Basin: from 'synform' to 'extensional' basins in the Tyrrhenian side of the Northern Apennines (Central Italy). Ital. J. Quaternary Sci. 10, 521-528.

Crouch, D.P., 1993. Water management in ancient Greek cities. New York: Oxford University Press.

Deiana, G., Pialli, G., 1994. The structural provinces of the Umbro-Marchean Apennines. Mem. Soc. Geol. It. 48, 473-484.

El-Qady, G., Hafez, M., Abdalla, M.A., and Ushijima, K., 2005. Imaging subsurface cavities using geoelectric tomography and ground-penetrating radar: J. Cave and Karst St. 67, 3, 174–181.

Gibson, P.J., Lyle, P., and George, D.M., 2004. Application of resistivity and magnetometry geophysical techniques for near-surface investigations in karstic terranes in Ireland. J. Cave and Karst St. 66, 2, 35–38.

Leeder, M.R., Gawthorpe, R.L., 1987. Sedimentary models for extensional tilt- lock/half graben basins. In Coward MP, Dewey JF, Hancock PL (eds.) Continental Extensional Tectonics: Geological Society of London, Special Publication 28, 139–152.

Loke, M.H., 2012. Tutorial: 2-D and 3-D Electrical Imaging Surveys. Geotomo Software, Malaysia (2012).

Margiotta, S., Negri, S., Parise, M., and Valloni, R., 2012. Mapping the susceptibility to sinkholes in coastal areas, based on stratigraphy, geomorphology and geophysics: Nat Hazards, 62, 2, 657–676. doi:10.1007/s11069-012-0100-1.

Morigi, A., 1997. Carsulae: topografia e monumenti. L'Erma di Bretschneider, Roma.

Captions

Figure 1- a) 3D model of the archaeological area of Carsulae obtained by Unhammed Aerial Veicle, are also indicated the two dolines with a dashed red line; b) Eastern tract of the deformed decumanus showing the sliding of road due to the doline collapse.

Figure 2 - a) Geologic sketch of the studied area: 1 - recent Holocene alluvial deposits; 2 - pelites, sands, conglomerates and filling deposits of the Tiber basin (Pliocene-Pleistocene); 3 – calcareous- marly and marly arenaceous-pelitic turbidites (Messinian); 4 - mainly calcareous rocks (Lias-Oligocene); 5-mainly tectonic features. b) Schematic geomorphological map of the area surrounding the Carsulae site.

Figure 3 - DEM map of Carsulae site and position of the geognostic borings and geophysical investigations carried out in the area (UTM projection, Zone 33 N, WGS84).

Figure 4 - Stratigraphic and lithological characterization of the geognostic borehole.

Figure 5- 2D resistivity sections of the interved ERT models

Figure 6 – Conductivity maps obtained by FDEM survey

Figure 7 – Comparison of FDEM and ERT results in the Roman Forum area

Figure 8 – Geophysical surveys conducted in the doline area: a) FDEM map with ERT and GPR profiles positions; b) ERT2 Profile; c) GPR1 Profile.

Figure 9 – Comparison between geophysical surveys conducted on the main road to access the site. a) Position of the profiles; b) ERT1 profile; c) GPR2 profile.

Table 1– Radiocarbon dating AMS.

Table 2 - ERT profile details.

Table 3- GPR profile details.

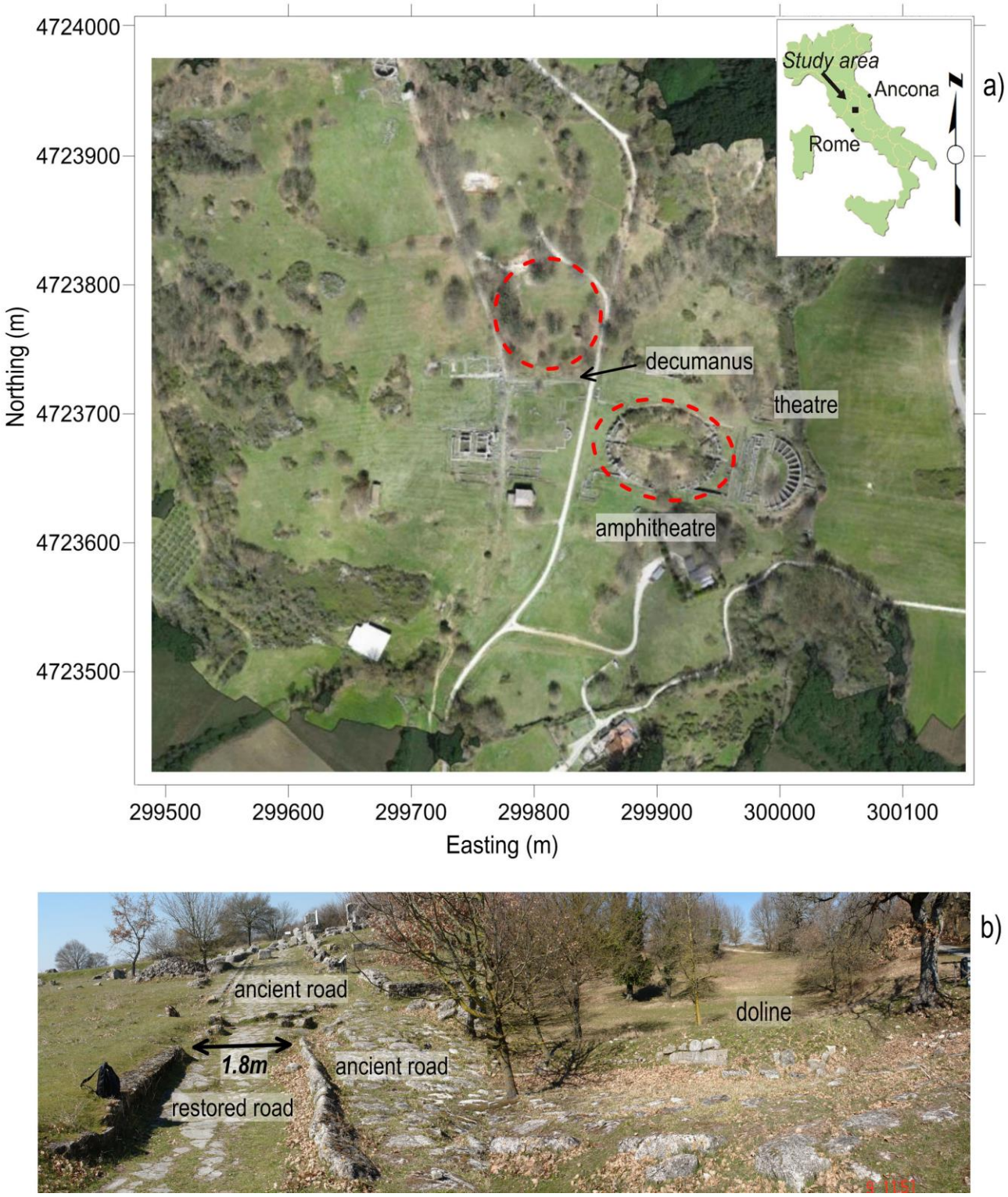
a)
Study area
Ancona
Rome
decumanus
theatre
amphitheatre
Northing (m)
4724000
4723900
4723800
4723700
4723600
4723500
Easting (m)
299500
299600
299700
299800
299900
300000
300100
b)
ancient road
1.8m
ancient road
restored road
doline

Figure 1

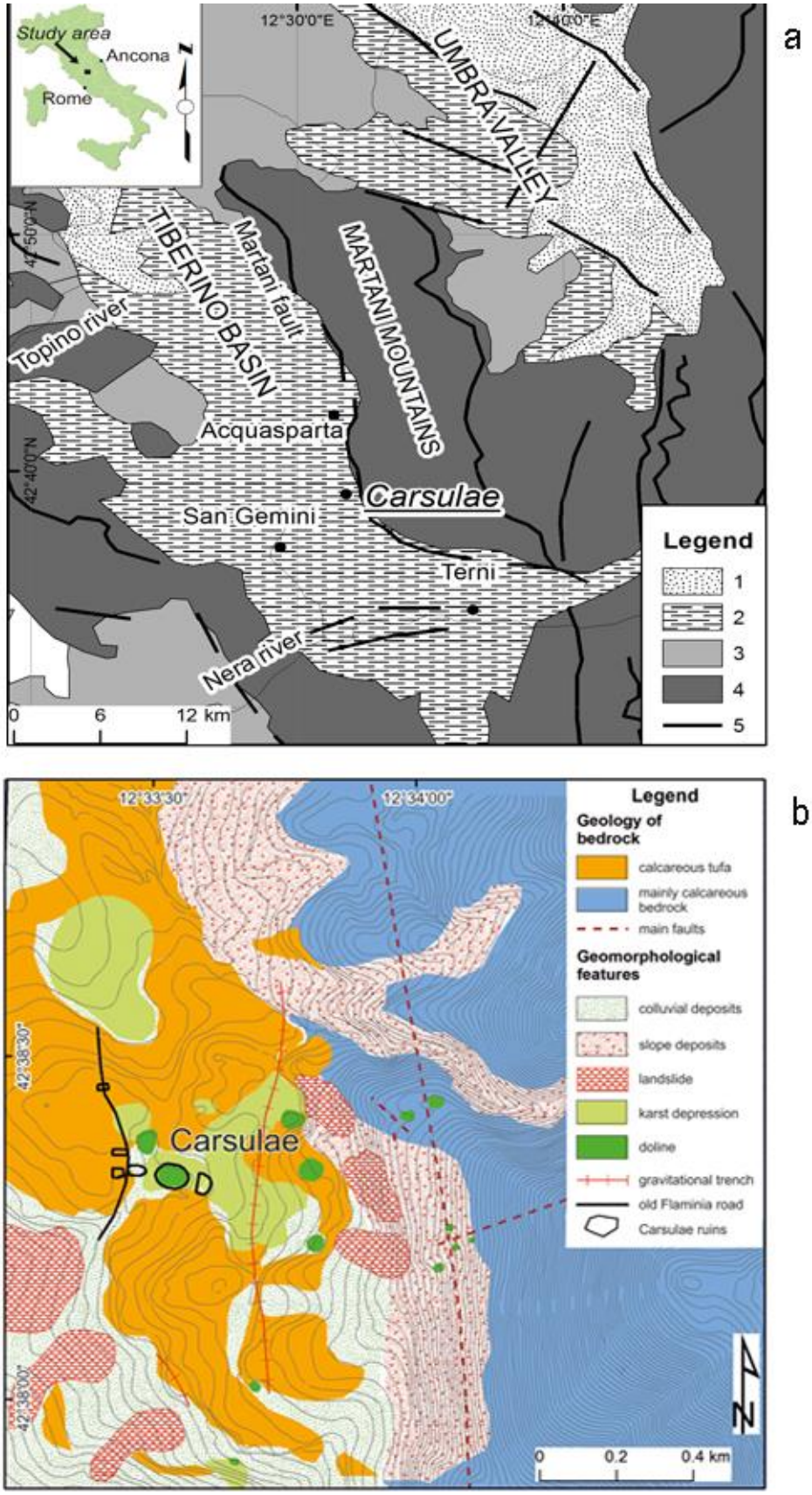
a
Study area
Ancona
Rome
12°30'0"E
12°40'0"E
UMBRA VALLEY
TIBERINO BASIN
Martani fault
MARTANI MOUNTAINS
Topino river
Acquasparta
Carsulae
San Gemini
Terni
Nera river
42°50'0"N
42°40'0"N
0
6
12 km
Legend
1
2
3
4
5
b
12°33'30"
12°34'00"
42°38'30"
42°38'00"
Carsulae
Legend
Geology of bedrock
calcareous tufa
mainly calcareous bedrock
main faults
Geomorphological features
colluvial deposits
slope deposits
landslide
karst depression
doline
gravitational trench
old Flaminia road
Carsulae ruins
N
0
0.2
0.4 km

Figure 2

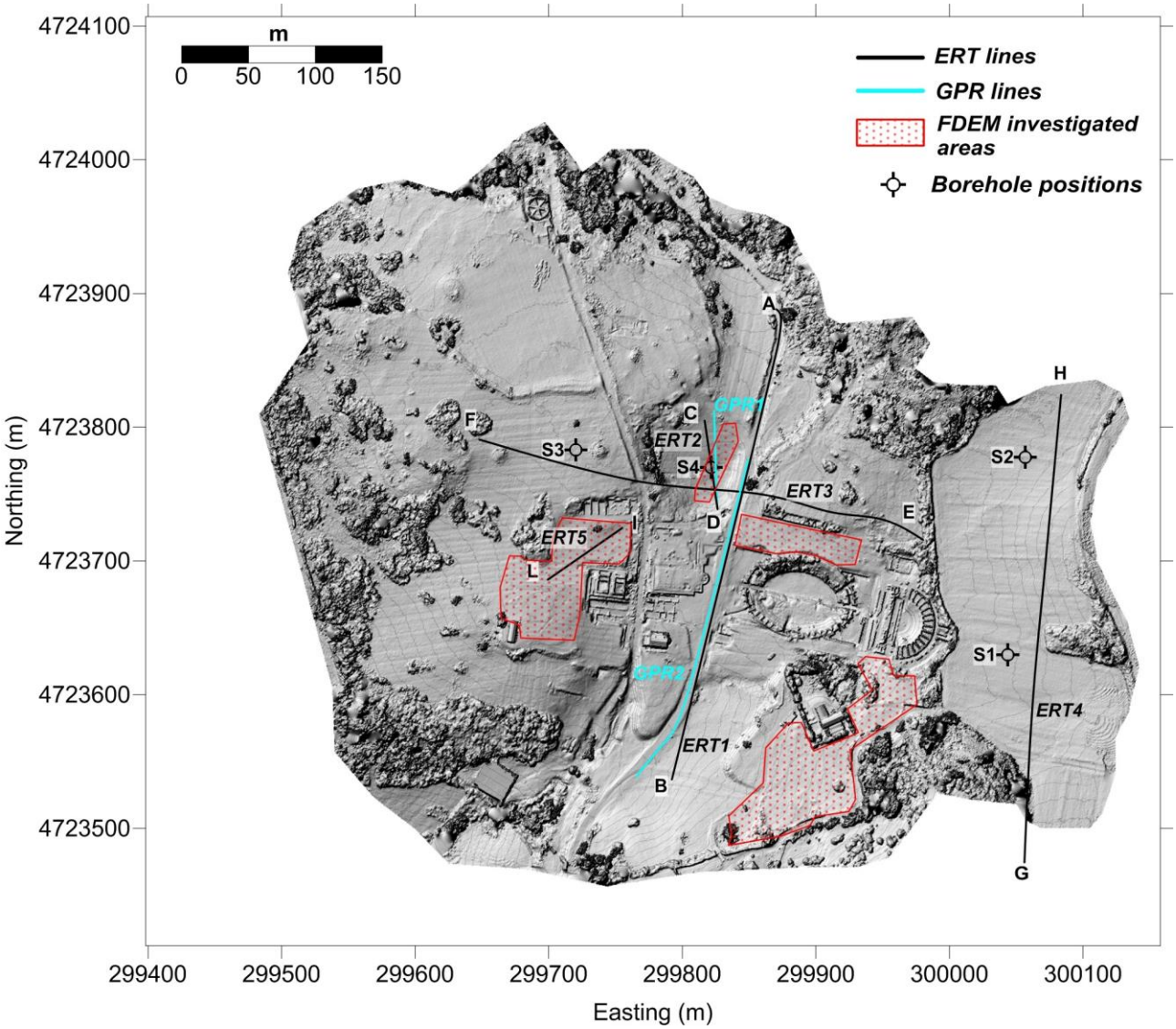
m
0
50
100
150
ERT lines
GPR lines
FDEM investigated areas
Borehole positions
A
B
C
D
E
F
G
H
I
L
ERT1
ERT2
ERT3
ERT4
ERT5
GPR1
GPR2
S1
S2
S3
S4
4724100
4724000
4723900
4723800
4723700
4723600
4723500
Northing (m)
299400
299500
299600
299700
299800
299900
300000
300100
Easting (m)

Figure 3

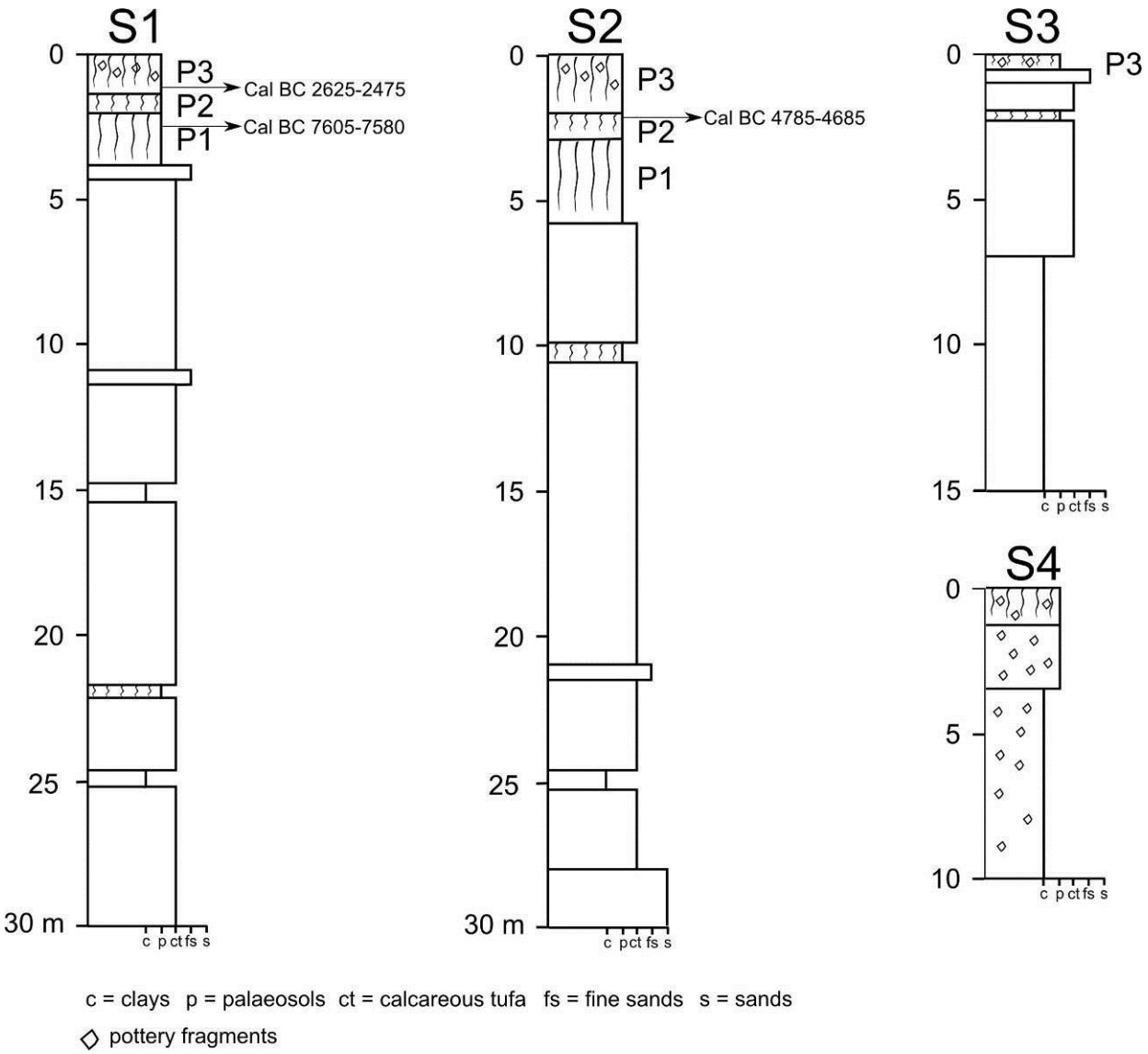
S1
S2
S3
S4
P3
P2
P1
Cal BC 2625-2475
Cal BC 7605-7580
Cal BC 4785-4685
0
5
10
15
20
25
30 m
c p ct fs s
c = clays p = palaeosols ct = calcareous tufa fs = fine sands s = sands
pottery fragments

Figure 4

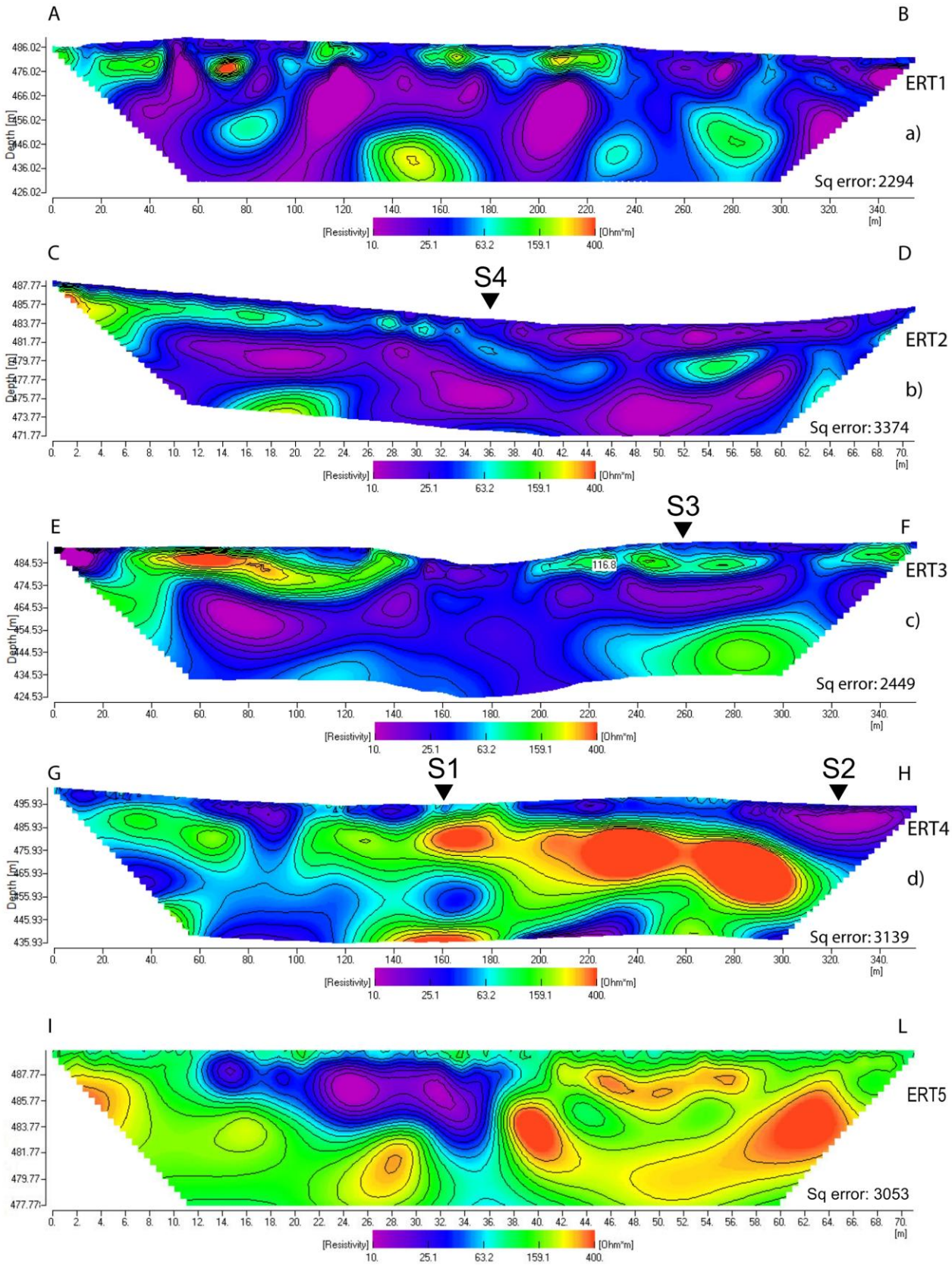
A
B
ERT1
a)
Sq error: 2294
C
D
S4
ERT2
b)
Sq error: 3374
E
S3
F
116.8
ERT3
c)
Sq error: 2449
G
S1
S2
H
ERT4
d)
Sq error: 3139
I
L
ERT5
Sq error: 3053
Depth [m]
[m]
[Resistivity]
[Ohm*m]
10.
25.1
63.2
159.1
400.

Figure 5

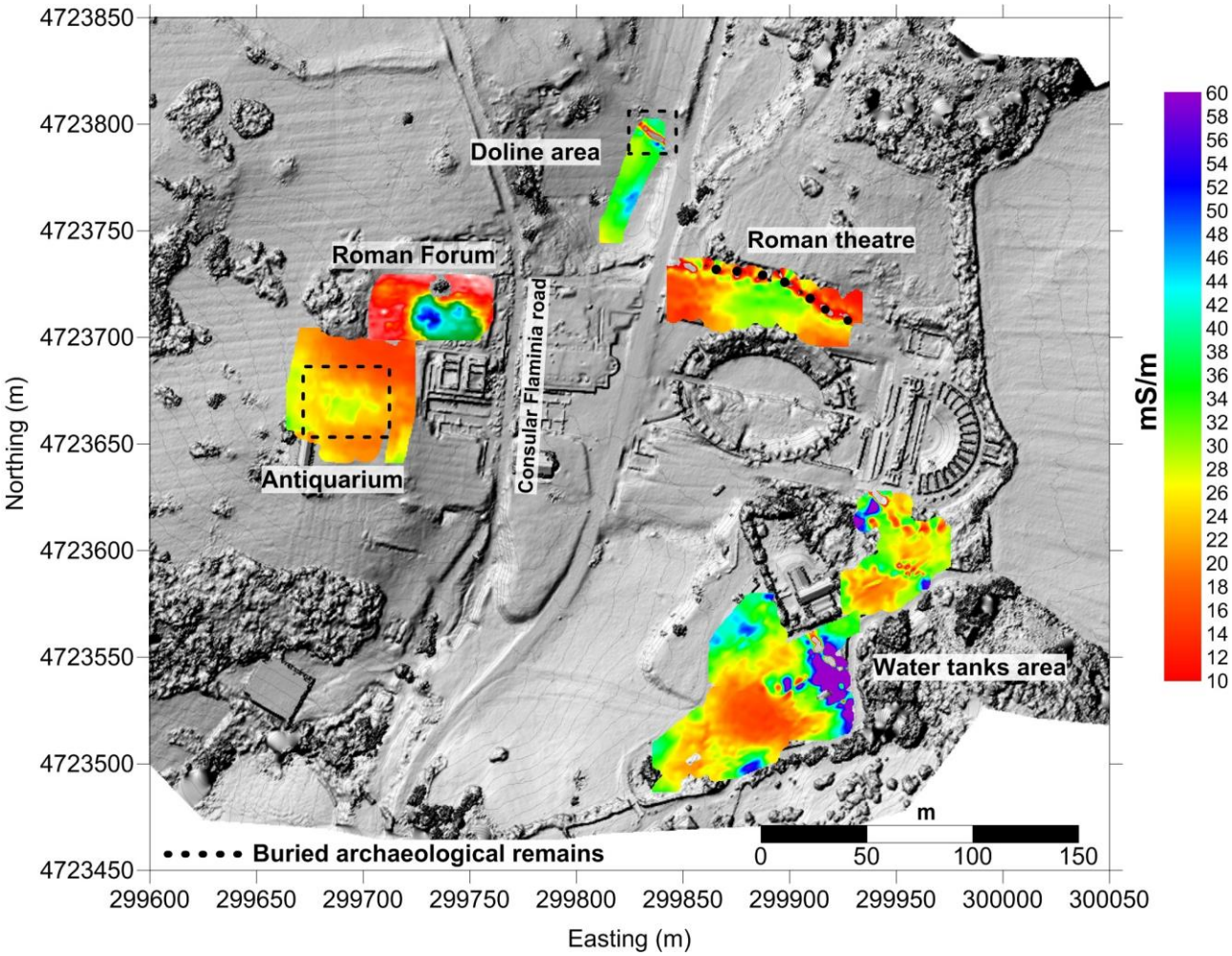
Doline area
Roman Forum
Roman theatre
Consular Flaminia road
Antiquarium
Water tanks area
Buried archaeological remains
m
0
50
100
150
Northing (m)
Easting (m)
4723850
4723800
4723750
4723700
4723650
4723600
4723550
4723500
4723450
299600
299650
299700
299750
299800
299850
299900
299950
300000
300050
mS/m
60
58
56
54
52
50
48
46
44
42
40
38
36
34
32
30
28
26
24
22
20
18
16
14
12
10

Figure 6

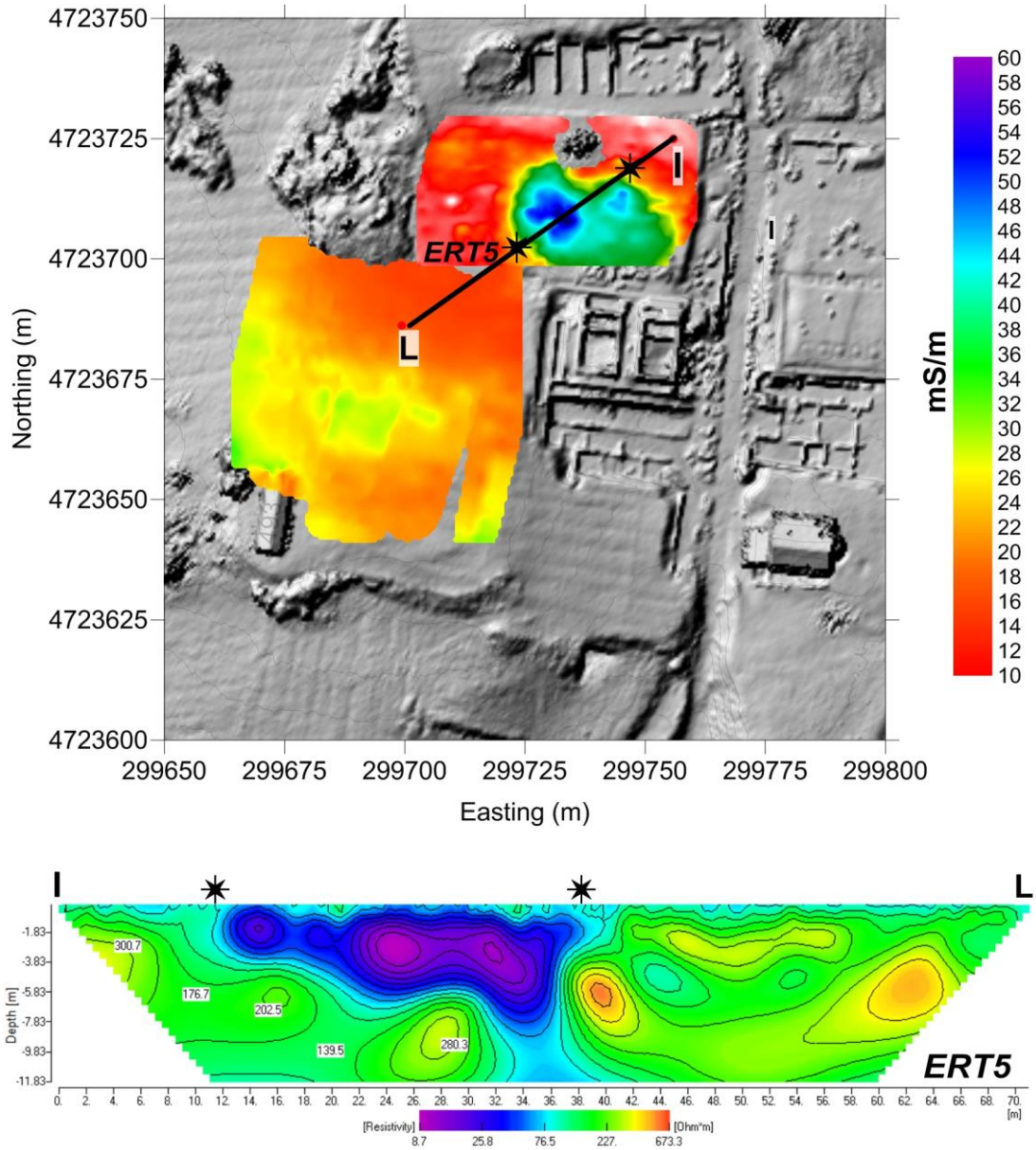
4723750
4723725
4723700
4723675
4723650
4723625
4723600
Northing (m)
299650
299675
299700
299725
299750
299775
299800
Easting (m)
ERT5
I
L
mS/m
60
58
56
54
52
50
48
46
44
42
40
38
36
34
32
30
28
26
24
22
20
18
16
14
12
10
I
L
ERT5
Depth [m]
-1.83
-3.83
-5.83
-7.83
-9.83
-11.83
300.7
176.7
202.5
139.5
280.3
[Resistivity]
[Ohm*m]
8.7
25.8
76.5
227.
673.3
[m]

Figure 7

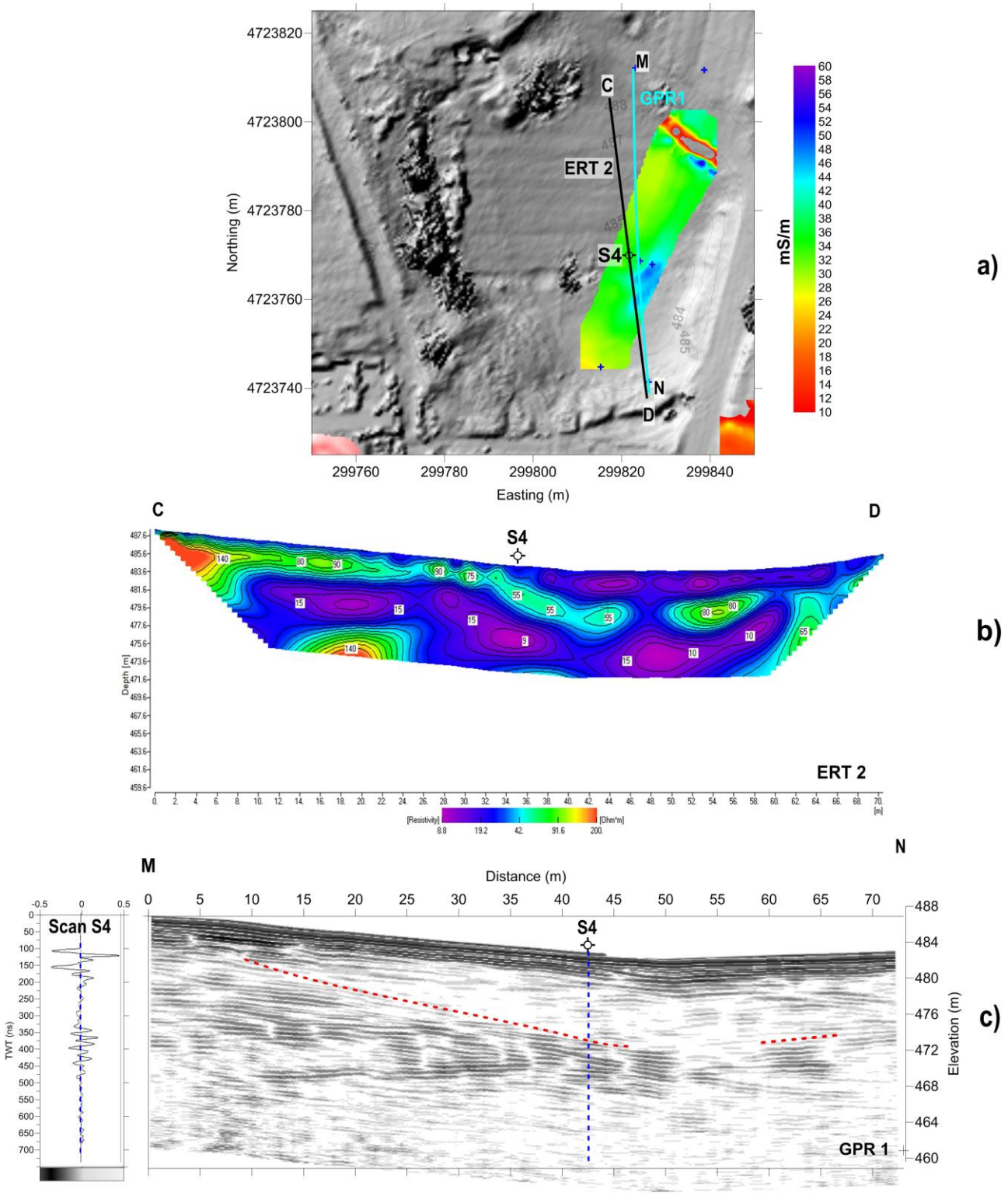
a)
Northing (m)
Easting (m)
mS/m
M
C
GPR1
ERT 2
S4
N
D
b)
C
D
S4
ERT 2
Depth [m]
c)
M
N
Distance (m)
Scan S4
S4
GPR 1
TWT (ns)
Elevation (m)

Figure 8

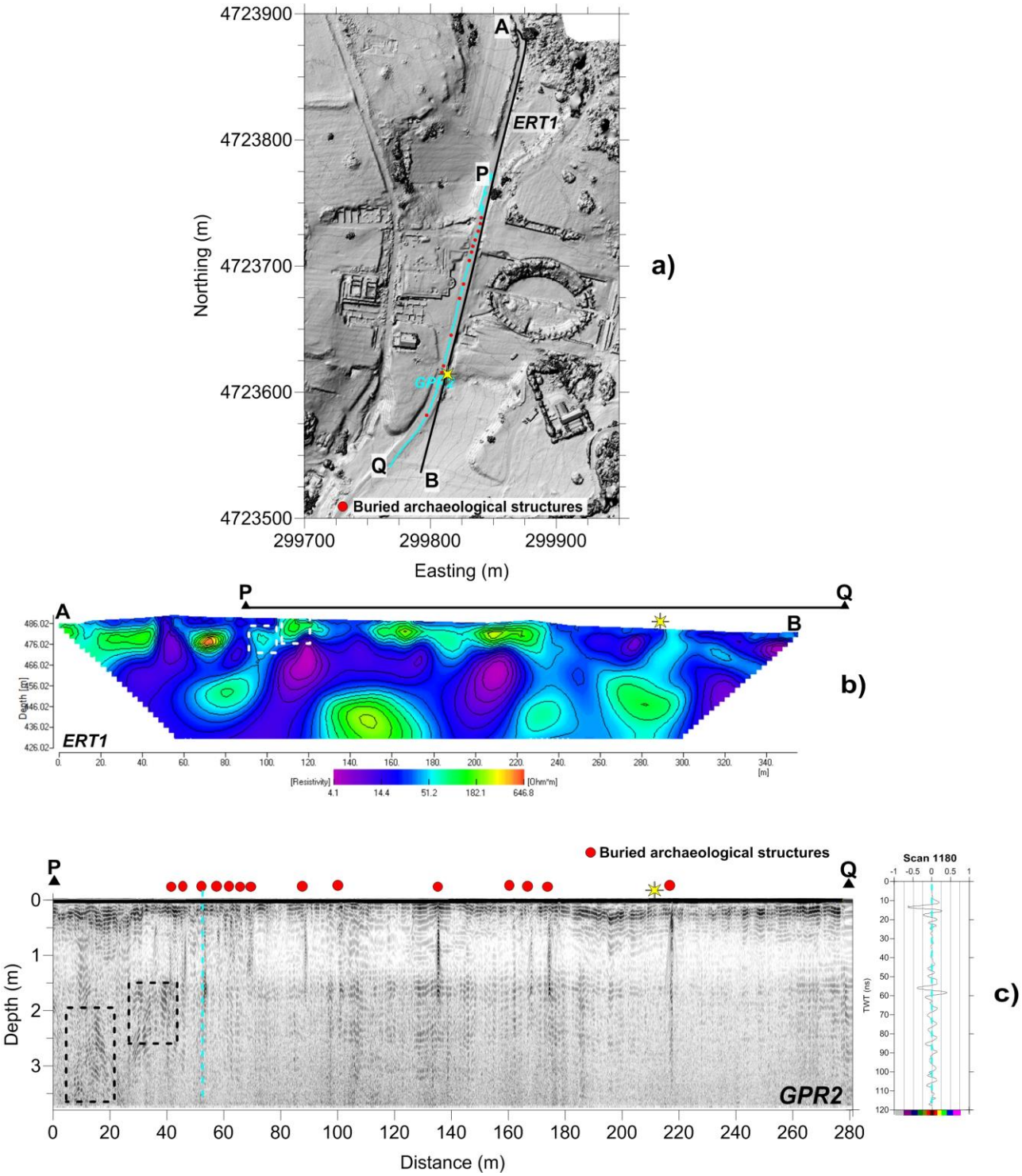
a)
A
ERT1
P
GPR2
Q
B
Buried archaeological structures
Northing (m)
Easting (m)
b)
ERT1
Depth [m]
[Resistivity]
[Ohm*m]
c)
Buried archaeological structures
GPR2
Depth (m)
Distance (m)
Scan 1180
TWT (ns)

Figure 9

Table 1

Sample ID	Depth (m)	Borehole	BETA Code	(Material) Pretreatment	Conventional Age	2 Sigma calibration
C1	1.4	S1	411539	(organic sediment): acid washes	8590 +/- 30 BP	Cal BC 7605 to 7580 (Cal BP 9555 to 9530)
C1/3	2.5	S1	411541	(organic sediment): acid washes	4040 +/- 30 BP	Cal BC 2830 to 2820 (Cal BP 4780 to 4770) and Cal BC 2625 to 2475 (Cal BP 4575 to 4425)
C2/2	2.1	S2	411540	(organic sediment): acid washes	5850 +/- 30 BP	Cal BC 4785 to 4685 (Cal BP 6735 to 6635) and Cal BC 4630 to 4620 (Cal BP 6580 to 6570)

Table 2

Profile name	Length (m)	Pseudo depth (m)	Electrodes	Electrodes spacing	Configuration	Injected current voltage (V)
ERT1	355	60	72	5 m	Wenner - Dipole dipole	800
ERT2	71	10	72	1 m	Wenner - Dipole dipole	800
ERT3	355	60	72	5 m	Wenner - Dipole dipole	800
ERT4	355	60	72	5 m	Wenner - Dipole dipole	800
ERT5	71	10	72	1 m	Wenner - Dipoledipole	800

Table 3

GPR profile	Length	Antenna frequency	Range	Investigation depth
GPR1	73 m	20 MHz	750 ns	24 m
GPR2	280 m	200 MHz	120 ns	3.7 m

Highlights

- Relationship between karstic phenomena and severe damages to some archaeological structures at Carsulae monumental site.
- Ground deformation related to the development of subsidence doline
- Understanding the evolution of this territory through an integrated geomorphological and geophysical approach.
- Acquisition of shallow and deep geological data for reconstructing the setting and thickness of the calcareous tufa basement on which the archaeological site stands.